Low-Frequency Scattering From Cylindrical Structures at Oblique Incidence

KAMAL SARABANDI AND THOMAS B. A. SENIOR, FELLOW, IEEE

Abstract—**Classical Rayleigh scattering theory is extended to the case of a homogeneous dielectric cylinder of arbitrary cross section whose transverse dimensions are much smaller than the wavelength. By assuming that the surface fields can be approximated by those of the infinite cylinder, the far zone scattered field is expressed in terms of polarizability tensors whose properties are discussed. Numerical results are presented for circular, semicircular, triangular, and square cylinders.**

I. Introduction

A KNOWLEDGE of the electromagnetic scattering properties of dielectric bodies is important in many areas of physics and engineering. For the remote sensing of terrain and vegetation, the scattering from a single leaf or twig is a key ingredient for most scattering models, and if the lateral dimensions of, for example, a leaf are large compared to the incident wavelength λ_0, it may be adequate to model it as a dielectric plate to which the physical optics approximation is applied [5]. At much lower frequencies and/or for smaller leaves whose dimensions are all small compared to λ_0, Rayleigh scattering theory is applicable [8]. The far zone scattered field is then attributable to induced electric and magnetic dipoles, and for plane wave incidence, the dependence on the direction and polarization of the incident field can be made explicit by introducing the electric and magnetic polarizability tensors [2]. The tensor elements are functions only of the geometry and material of the scatterer, and are expressible as weighted surface integrals of certain potentials which can be obtained from the solutions of elementary integral equations.

An intermediate situation is provided by a pine needle whose transverse dimensions are small compared to the wavelength, but whose length is much greater than λ_0. This is the case which is treated here. For a plane wave incident obliquely on a homogeneous dielectric cylinder of infinite length, it is shown that the field at any point outside the cylinder can be written as the sum of contributions from line dipoles whose moments per unit length are expressible in terms of polarizability tensors. Integral equations are derived from which to determine the tensor elements, and results are presented for a variety of cylinders and material constants. The generalization to a cylinder of finite length is now trivial. In accordance with the physical optics approximation, it is assumed that the surface field is the same as that on the infinite cylinder, leading immediately to an expression for the far field in terms of the same polarizability tensors. The results are applicable to the remote sensing of twigs, stalks, and vegetation needles at centimeter and millimeter wavelengths.

Manuscript received June 13, 1989; revised December 12, 1989. This work was supported by the NASA EOS Simultaneity Project.

The authors are with the Radiation Laboratory, Department of Electrical Engineering and Computer Science, University of Michigan, Ann Arbor, MI 48109.

IEEE Log Number 9037451.

II. Infinite Cylinders

A homogeneous dielectric cylinder of arbitrary cross section is oriented with its generators parallel to the z axis of a cartesian coordinate system x, y, z (see Fig. 1). The relative permittivity and permeability of the dielectric are ϵ and μ, respectively, and the cylinder is illuminated by the linearly polarized plane wave

$$\boldsymbol{E}^i = \hat{a}\, e^{ik_0 \hat{k}^i \cdot \bar{r}} \qquad \boldsymbol{H}^i = Y_0 \hat{b}\, e^{ik_0 \hat{k}^i \cdot \bar{r}} \tag{1}$$

propagating in the direction

$$\hat{k}^i = \hat{x} \sin\beta \cos\phi_0 + \hat{y} \sin\beta \sin\phi_0 + \hat{z} \cos\beta. \tag{2}$$

The unit vectors $\hat{a}$ and $\hat{b}$ specifying the directions of the incident electric and magnetic fields are such that

$$\hat{a} \times \hat{b} = \hat{k}^i, \qquad \hat{k}^i \cdot \hat{a} = \hat{k}^i \cdot \hat{b} = 0$$

and k_0 and Y_0 ($= 1/Z_0$) are the propagation constant and intrinsic admittance, respectively, of the surrounding free space medium. A time factor $e^{-i\omega t}$ has been assumed and suppressed.

Since the cylinder is uniform in the z direction, the scattered field must have the same z dependence as the incident field, namely $e^{ik_0 z \cos\beta}$. If, for brevity, this factor is omitted, the electric and magnetic Hertz vectors defining the scattered field can be written as

$$\Pi^e(x, y) = \frac{-Z_0}{4k_0} \int_S \boldsymbol{J}^e(x', y') \cdot H_0^{(1)}\left(k_0 \sin\beta \sqrt{(x - x')^2 + (y - y')^2}\right) \cdot dx'\, dy' \tag{3}$$

$$\Pi^m(x, y) = \frac{-Y_0}{4k_0} \int_S \boldsymbol{J}^m(x', y') \cdot H_0^{(1)}\left(k_0 \sin\beta \sqrt{(x - x')^2 + (y - y')^2}\right) \cdot dx'\, dy' \tag{4}$$

0196-2892/90/0900-0879$01.00 © 1990 IEEE

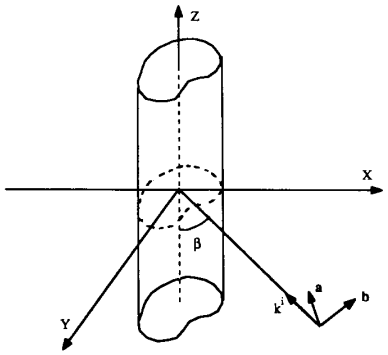

Fig. 1. Geometry of the infinite cylinder in the x, y, z coordinate system.

where $\boldsymbol{J}^e$ and $\boldsymbol{J}^m$ are the induced electric and magnetic currents, $H_0^{(1)}$ is the Hankel function of the first kind of zeroth order, and the integration is over the cross section S of the cylinder. In terms of the Hertz vectors, the scattered fields are [7, p. 31]

$$\boldsymbol{E}^s = \nabla\nabla \cdot \Pi^e + k_0^2\Pi^e + ik_0Z_0\nabla \times \Pi^m$$
$$\boldsymbol{H}^s = \nabla\nabla \cdot \Pi^m + k_0^2\Pi^m + ik_0Y_0\nabla \times \Pi^e \quad (5)$$

and we note that

$$\nabla = \nabla_t + ik_0 \cos\beta\hat{z} \quad (6)$$

where ∇_t is the transverse operator which, in cartesian coordinates, is

$$\nabla_t = \hat{x}\frac{\partial}{\partial x} + \hat{y}\frac{\partial}{\partial y}.$$

If d is a typical transverse dimension of the cylinder and k_0d, $k_0|N|d << 1$ where $N = (\epsilon\mu)^{1/2}$ is the refractive index, the currents and the Hertz vectors can be approximated by the lowest order terms in their representations for small k_0 (see (13)), whereas for the Hankel function, the leading term involves $\ln k_0$. When these are substituted into (3) and (4), and hence (5), the scattered field in the near field of the cylinder can be written as

$$\boldsymbol{E}^s = \nabla_t\nabla_t \cdot \Pi^e + O(k_0)$$
$$\boldsymbol{H}^s = \nabla_t\nabla_t \cdot \Pi^m + O(k_0) \quad (7)$$

implying

$$E_z^s = H_z^s = 0.$$

Thus, at low frequencies, the electric and magnetic fields decouple, with the scattered electric field determined by the electric current (and hence, permittivity) alone, and the magnetic field by the magnetic current (and permeability). Since the solution for the magnetic field can be deduced from that for the electric field by replacing ϵ and $\hat{a}$ by μ and $Y_0\hat{b}$, respectively, it is now sufficient to take $\mu = 1$ corresponding to a nonmagnetic dielectric.

To determine the static field, the Hankel function in (3) is replaced by its small argument expansion:

$$H_0^{(1)}(k_0 \sin\beta|\bar{\rho} - \bar{\rho}'|) \approx 1 + \frac{i2}{\pi}\gamma + \frac{i2}{\pi}\ln(k_0 \sin\beta|\bar{\rho} - \bar{\rho}'|)$$

where $\bar{\rho}$ is the two-dimensional position vector and $\gamma = 0.5772157\cdots$ is Euler's constant. On inserting this into (7) and noting that

$$\nabla_t \ln(k_0 \sin\beta|\bar{\rho} - \bar{\rho}'|) = \nabla_t \ln|\bar{\rho} - \bar{\rho}'|$$

independent of k_0, the lowest order scattered field becomes

$$\boldsymbol{E}^s(\bar{\rho}) = -\nabla_t\left\{\frac{iZ_0}{2\pi k_0}\int_S \boldsymbol{J}_t^e(\bar{\rho}') \cdot \nabla_t \ln|\bar{\rho} - \bar{\rho}'|\, ds'\right\}$$

with

$$\boldsymbol{J}_t^e(\bar{\rho}) = J_x^e(\bar{\rho})\hat{x} + J_y^e(\bar{\rho})\hat{y}.$$

Since $(i/\omega)\boldsymbol{J}_t^e = \boldsymbol{P}$ is simply the dipole moment per unit area [7, p. 184], it follows that

$$\boldsymbol{E}^s = -\nabla_t\Phi^s(\bar{\rho}) \quad (8)$$

where

$$\Phi^s(\bar{\rho}) = \frac{iZ_0}{2\pi k_0}\int_S \boldsymbol{J}_t^e(\bar{\rho}') \cdot \nabla_t \ln|\bar{\rho} - \bar{\rho}'|\, ds' \quad (9)$$

is the two-dimensional electrostatic potential.

To the zeroth order in k_0, the incident electric field, is

$$\boldsymbol{E}^i = \hat{a} = a_x\hat{x} + a_y\hat{y} + a_z\hat{z}$$

which can be written as

$$\boldsymbol{E}^i = -\nabla_t\Phi^i + a_z\hat{z} \quad (10)$$

with

$$\Phi^i = -a_x(x + c_1) - a_y(y + c_2) \quad (11)$$

where c_1, c_2 are arbitrary constants. The total potential is then

$$\Phi = \Phi^i + \Phi^s$$

and the dependence on $\hat{a}$ can be made explicit by writing

$$\Phi = a_x\Phi_1 + a_y\Phi_2 \quad (12)$$

with a similar decomposition for Φ^i and Φ^s.

In terms of the total field, the polarization current is

$$\boldsymbol{J}^e(\bar{\rho}) = -ik_0Y_0(\epsilon - 1)(\boldsymbol{E}^i + \boldsymbol{E}^s) \quad (13)$$

and since $E_z^s = 0$,

$$J_z^e(\bar{\rho}) = -ik_0Y_0(\epsilon - 1)a_z \quad (14)$$

in agreement with the result of Van Bladel [9]. Also,

$$\boldsymbol{J}_t^e(\bar{\rho}) = -ik_0Y_0(\epsilon - 1)(a_x\hat{x} + a_y\hat{y} - \nabla_t\Phi^s)$$

that is,

$$\boldsymbol{J}_t^e(\bar{\rho}) = ik_0Y_0(\epsilon - 1)\nabla_t(a_x\Phi_1 + a_y\Phi_2) \quad (15)$$

and the derivation and solution of integral equations for Φ_1 and Φ_2 are discussed in Section IV.

III. Polarizability Tensors

At large distances $\rho >> k_0 d^2$ from the cylinder, the Hankel function in the expressions (3), (4) for Π^e, Π^m can be replaced by its large argument expansion. Thus,

$$\Pi^e \approx -\frac{Z_0}{4k_0}\sqrt{\frac{2}{\pi k_0 \rho \sin\beta}} \cdot \exp\left(ik_0(\rho \sin\beta + z\cos\beta) - i\frac{\pi}{4}\right) \cdot \int_S \boldsymbol{J}^e(\bar{\rho}')\, ds'$$

$$= \frac{i}{4}\sqrt{\frac{2}{\pi k_0 \rho \sin\beta}} \cdot \exp\left(ik_0(\rho \sin\beta + z\cos\beta) - i\frac{\pi}{4}\right)(\epsilon - 1) \cdot \int_S \left\{-\nabla_t(a_x\Phi_1 + a_y\Phi_2) + a_z\hat{z}\right\} ds' \quad (16)$$

in which the z dependence has been restored, and since

$$\int_S \nabla_t' \Phi(\bar{\rho}')\, ds' = \int_C \Phi(\bar{\rho}')\hat{n}'\, dc'$$

where $\hat{n}$ is the outward unit vector normal to the boundary C of S,

$$\Pi^e = \frac{i}{4}\sqrt{\frac{2}{\pi k_0 \rho \sin\beta}} \cdot \exp\left(ik_0(\rho \sin\beta + z\cos\beta) - i\frac{\pi}{4}\right)(\epsilon - 1) \cdot \left\{-\int_C (a_x\Phi_1 + a_y\Phi_2)\hat{n}'\, dc' + Aa_z\hat{z}\right\} \quad (17)$$

where A is the cross-sectional area of the cylinder.

Similarly, if Ψ is the total magnetostatic potential such that

$$\boldsymbol{H} = -Y_0\nabla_t\Psi + Y_0 b_z\hat{z}$$

with

$$\Psi = b_x\Psi_1 + b_y\Psi_2$$

we have

$$\Pi^m = \frac{i}{4}\sqrt{\frac{2}{\pi k_0 \rho \sin\beta}} \cdot \exp\left(ik_0(\rho \sin\beta + z\cos\beta) - i\frac{\pi}{4}\right)(\mu - 1) \cdot \left\{-\int_C (b_x\Psi_1 + b_y\Psi_2)\hat{n}'\, dc' + Ab_z\hat{z}\right\} \quad (18)$$

and from the z dependence in (17) and (18), it is evident that the scattering is confined to the forward cone $\hat{k}^s \cdot \hat{z} = \cos\beta$. In the far zone, $\nabla \approx ik_0\hat{k}^s$, and hence,

$$\boldsymbol{E}^s = \sqrt{\frac{2}{\pi k_0 \rho \sin\beta}} \cdot \exp\left(ik_0(\rho \sin\beta + z\cos\beta) - i\frac{\pi}{4}\right)\boldsymbol{S}$$

with

$$\boldsymbol{S} = -\frac{ik_0^2}{4}\left\{\hat{k}^s \times \hat{k}^s \times (\epsilon - 1) \cdot \left[-\int_C (a_x\Phi_1 + a_y\Phi_2)\hat{n}'\, dc' + Ab_z\hat{z}\right] + \hat{k}^s \times (\mu - 1) \cdot \left[-\int_C (b_x\Psi_1 + b_y\Psi_2)\hat{n}'\, dc' + Ab_z\hat{z}\right]\right\}. \quad (19)$$

The scattering is attributable to electric and magnetic line dipoles along the z axis. The electric dipole moment per unit length is

$$\boldsymbol{p} = \epsilon_0(\epsilon - 1)\left\{-\int_C (a_x\Phi_1 + a_y\Phi_2)\hat{n}'\, dc' + Ab_z\hat{z}\right\} \quad (20)$$

and if

$$\boldsymbol{p} = \epsilon_0 \boldsymbol{P} \cdot \hat{a}, \quad (21)$$

the elements of the polarizability tensor $\boldsymbol{P}$ are

$$P_{xx} = -(\epsilon - 1)\int_C \Phi_1\hat{n}' \cdot \hat{x}\, dc'$$

$$P_{xy} = -(\epsilon - 1)\int_C \Phi_2\hat{n}' \cdot \hat{x}\, dc'$$

$$P_{yx} = -(\epsilon - 1)\int_C \Phi_1\hat{n}' \cdot \hat{y}\, dc'$$

$$P_{yy} = -(\epsilon - 1)\int_C \Phi_2\hat{n}' \cdot \hat{y}\, dc'$$

$$P_{zz} = (\epsilon - 1)A$$

$$P_{xz} = P_{zx} = P_{yz} = P_{zy} = 0. \quad (22)$$

The elements are functions only of the geometry and permittivity of the cylinder and are real if ϵ is. Using reciprocity, it can be shown that the tensor is symmetric, i.e., $P_{yx} = P_{xy}$ and if the cylinder is symmetric about either the x or y axis, the tensor is diagonal ($P_{yx} = P_{xy} = 0$) in the given coordinate system.

Similarly, the magnetic dipole moment per unit length is

$$\boldsymbol{m} = Y_0(\mu - 1)\left\{-\int_C (b_x\Psi_1 + b_y\Psi_2)\hat{n}'\, dc' + Ab_z\hat{z}\right\}$$

and if[1]

$$\boldsymbol{m} = Y_0 \boldsymbol{M} \cdot \hat{b}$$

the magnetic polarizability tensor $\boldsymbol{M}$ differs from $\boldsymbol{P}$ only in having μ and Ψ in place of ϵ and Φ. Clearly, for a nonmagnetic dielectric, $\boldsymbol{m} = 0$. In terms of the tensors,

$$\boldsymbol{S} = -\frac{ik_0^2}{4}\left\{\hat{k}^s \times \hat{k}^s \times [\boldsymbol{P} \cdot \hat{a}] + \hat{k}^s \times [\boldsymbol{M} \cdot \hat{b}]\right\} \tag{23}$$

and since $\boldsymbol{P}$ and $\boldsymbol{M}$ are accurate to the zeroth order in k_0, the terms omitted from the expression for $\boldsymbol{S}$ are $O(k_0^3, k_0^4 \ln k_0)$. Equation (23) makes explicit the dependence on the incident and scattered field directions.

IV. Tensor Elements

To compute the tensor elements, it is necessary to determine the potential on the boundary C, and one way to do this is using integral equations. For brevity, we shall confine attention to the electrostatic potential Φ_1.

From (9) and (15), the scattered field potential is

$$\Phi_1^s(\bar{\rho}) = \frac{\epsilon - 1}{2\pi}\int_S \nabla_t' \Phi_1(\bar{\rho}\,') \cdot \nabla_t' \ln|\bar{\rho} - \bar{\rho}\,'|\, ds'$$

and since

$$\begin{aligned}\nabla_t' \Phi_1(\bar{\rho}\,') \cdot \nabla_t' \ln|\bar{\rho} - \bar{\rho}\,'| &= \nabla_t' \cdot \left(\Phi_1(\bar{\rho}\,')\nabla_t' \ln|\bar{\rho} - \bar{\rho}\,'|\right) \\ &\quad - \Phi_1(\bar{\rho}\,')\nabla_t'^2 \ln|\bar{\rho} - \bar{\rho}\,'|\end{aligned}$$

we have

$$\Phi^s(\bar{\rho}) = \frac{\epsilon - 1}{2\pi}\int_C \nabla_t' \Phi_1(\bar{\rho}\,') \cdot \frac{\partial}{\partial n'} \ln|\bar{\rho} - \bar{\rho}\,'|\, dc' - \frac{\epsilon - 1}{2\pi}\Delta$$

where

$$\Delta = \int_S \Phi_1(\bar{\rho}\,')\nabla_t'^2 \ln|\bar{\rho} - \bar{\rho}\,'|\, ds'.$$

When the observation point is on the boundary, the boundary condition gives

$$\Phi_1^s = \Phi_1 + x + c_1$$

and for a piecewise smooth surface, $\Delta = \alpha\Phi_1(\bar{\rho})$ where α is equal to the angle subtended by the surface at the point $\bar{\rho}$. Thus for a smooth surface, $\alpha = \pi$, and an integral equation for Φ_1 on C is then

$$\left(\frac{\epsilon + 1}{2}\right)\Phi_1(\bar{\rho}) - \left(\frac{\epsilon - 1}{2\pi}\right)\int_C \Phi_1(\bar{\rho}\,')\frac{\cos\theta'}{|\bar{\rho} - \bar{\rho}\,'|}\, dc' = -x - c_1 \tag{24}$$

where θ' is shown in Fig. 2.

One of the few geometries for which an analytical solution of (24) is possible is a circular cylinder. If the radius is r,

$$\frac{\cos\theta'}{|\bar{\rho} - \bar{\rho}\,'|} = \frac{1}{2r}$$

independent of position on C. The integral on the left-hand side of (24) is therefore independent of $\bar{\rho}$, which forces $\Phi_1(\bar{\rho}\,')$ to be a linear function of x independent of y. By simple substitution, it is found that

$$\Phi_1(\bar{\rho}\,') = -\frac{2x}{\epsilon + 1} - c_1$$

and hence,

$$\frac{P_{xx}}{A} = \frac{P_{yy}}{A} = 2\frac{\epsilon - 1}{\epsilon + 1} \tag{25}$$

with

$$\frac{P_{zz}}{A} = \epsilon - 1. \tag{26}$$

These are consistent with the eigenfunction expansion for a homogeneous cylinder at oblique incidence [4] when only two terms in the series are retained, and are identical to the tensor elements for a long thin spheroid when normalized to the volume [6]. For $\epsilon = \epsilon' + i\epsilon''$, the real and imaginary parts of P_{xx}/A [see (25)] are plotted as functions of ϵ' for a variety of ϵ'' in Figs. 3 and 4, respectively.

With other geometries, it is a trivial matter to solve the integral equation numerically, and a moment method code has been developed for this purpose. The contour is divided into N segments small enough to treat the potential as constant over each, and point matching is then employed to convert the equation into a set of N linear equations of the form:

$$\mathcal{Z}\mathfrak{X} = \mathcal{Y} \tag{27}$$

where $\mathcal{Z}$ is the impedance matrix, $\mathfrak{X}$ is the potential (unknown) vector, and $\mathcal{Y}$ is the excitation (known) vector.

[1] $\boldsymbol{M}$ differs in sign from the magnetic polarizability tensor usually defined (see, for example, Keller *et al.* [1]).

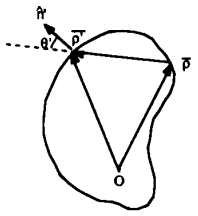

Fig. 2. Geometry of an arbitrary cylinder in the transverse plane.

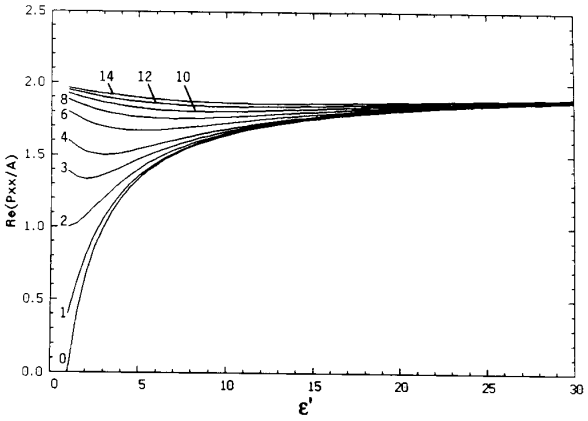

Fig. 3. Real part of normalized polarizability tensor element P_{xx}/A for a circular cylinder.

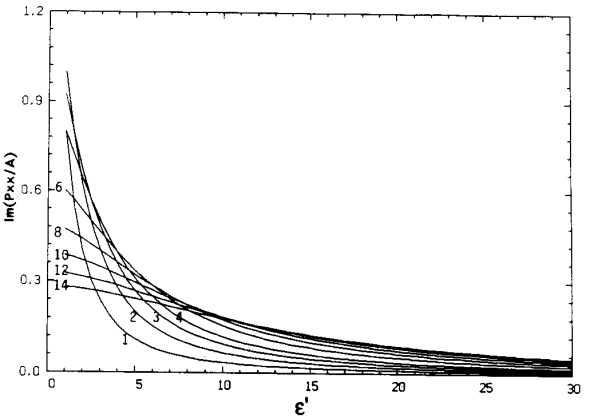

Fig. 4. Imaginary part of the normalized polarizability tensor element P_{xx}/A for a circular cylinder.

The elements of the impedance matrix are

$$Z_{mn} = \begin{cases} -\dfrac{\epsilon - 1}{2\pi} \dfrac{\Delta_n \cos \theta_{mn}}{\sqrt{(x_m - x_n)^2 + (y_m - y_n)^2}}, \\ \qquad m \neq n \\ \dfrac{\epsilon + 1}{2}, \qquad m = n \end{cases} \tag{28}$$

where Δ_n is the length of the nth segment.

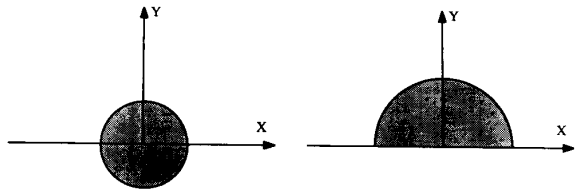

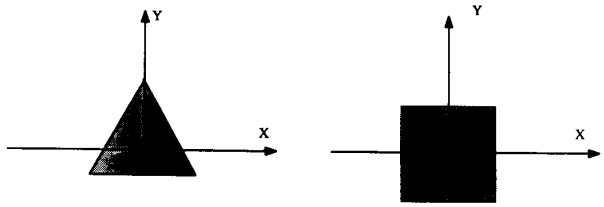

Fig. 5. Geometry of the cross section of circular, semicircular, triangular, and square cylinders.

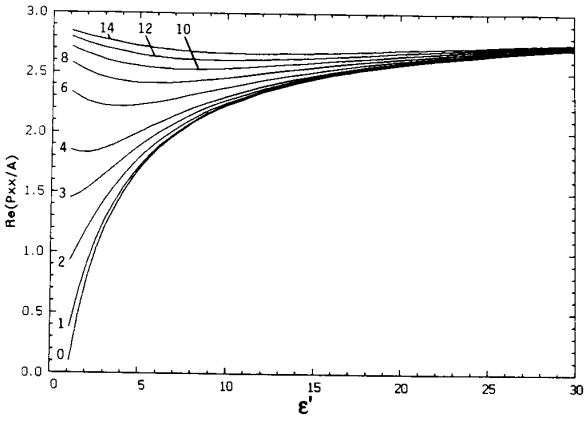

Fig. 6. Real part of the normalized polarizability tensor element P_{xx}/A for a semicircular cylinder.

The tensor elements have been computed for cylinders whose cross sections are the semicircle, equilateral triangle, and square shown in Fig. 5, and in each case, symmetry about the y axis diagonalizes the tensor. In Figs. 6–9, the real and imaginary parts of P_{xx}/A and P_{yy}/A for the semicircular cylinder are plotted as functions of ϵ'. Qualitatively, the curves are similar to those for the circular cylinder, and this prompted a search for simple analytical formulas. Since the scattering vanishes if $\epsilon = 1$ and the integral equation (25) shows that the potential is infinite if $\epsilon = -1$, it was assumed that (for example)

$$\frac{P_{xx}}{A} = c_0 \frac{\epsilon - 1}{\epsilon + 1} \cdot \frac{\epsilon + c_1}{\epsilon + c_2}$$

where c_0, c_1, and c_2 are constants, and after a few trials, an excellent fit to the data was obtained with the empirical formulas

$$\frac{P_{xx}}{A} = 3.00 \frac{\epsilon - 1}{\epsilon + 1} \cdot \frac{\epsilon + 1.05}{\epsilon + 2.20} \tag{29}$$

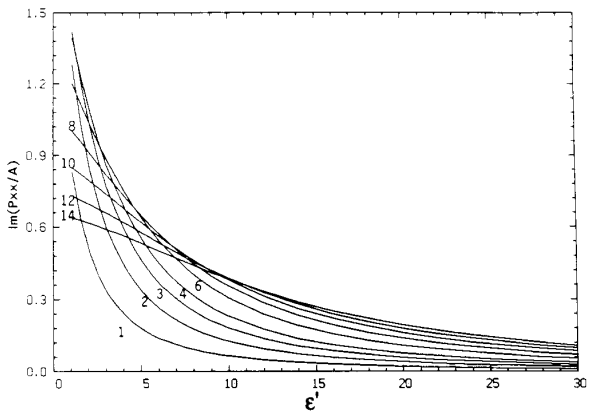

Fig. 7. Imaginary part of the normalized polarizability tensor element P_{xx}/A for a semicircular cylinder.

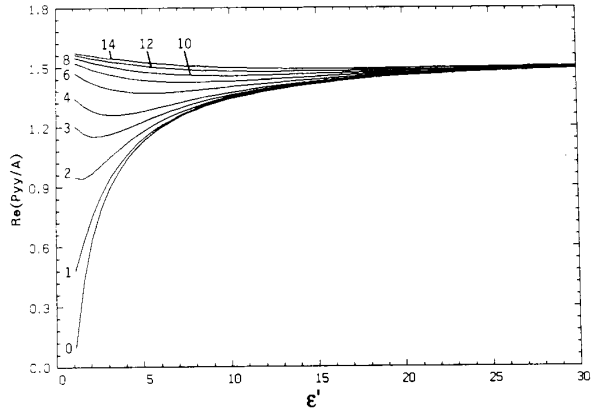

Fig. 8. Real part of the normalized polarizability tensor element P_{yy}/A for a semicircular cylinder.

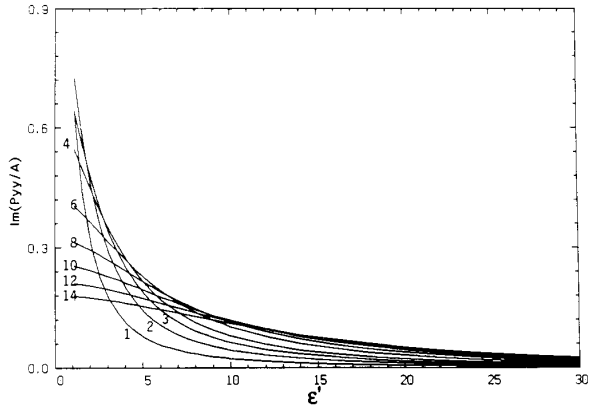

Fig. 9. Imaginary part of the normalized polarizability tensor element P_{yy}/A for a semicircular cylinder.

$$\frac{P_{yy}}{A} = 1.56\,\frac{\epsilon - 1}{\epsilon + 1} \cdot \frac{\epsilon + 2.60}{\epsilon + 2.00}. \tag{30}$$

The error is less than 2%. The analogous results for the triangular and square cylinders are

$$\frac{P_{xx}}{A} = \frac{P_{yy}}{A} = 2.64\,\frac{\epsilon - 1}{\epsilon + 1} \cdot \frac{\epsilon + 4.17}{\epsilon + 5.95} \tag{31}$$

and

$$\frac{P_{xx}}{A} = \frac{P_{yy}}{A} = 2.16\,\frac{\epsilon - 1}{\epsilon + 1} \cdot \frac{\epsilon + 3.38}{\epsilon + 3.76}, \tag{32}$$

respectively, and the latter agree with the values reported by Mei and Van Bladel [3].

V. Finite Cylinder

For a cylinder of finite length $l >> \lambda_0$, a method that is widely used to compute the scattered field is the physical optics approximation [4]. This assumes that the surface fields are those of the infinite cylinder, and although the conditions for its validity are difficult to determine, comparison to numerical data has shown that at least the dominant features of the scattering patterns are accurately reproduced. To determine the far field, the three-dimensional Green's function is employed in place of the Hankel function. The scattering is no longer confined to the forward cone, and if, as before, the scattering direction is $\hat{k}^s$, the integration with respect to z can be carried out immediately and gives $(l \sin U)/U$ where

$$U = \frac{k_0 l}{2}(\hat{k}^s \cdot \hat{z} - \cos\beta). \tag{33}$$

The far-field amplitude, defined as the coefficient of $re^{-ik_0 r}\boldsymbol{E}^s$ in the far zone, is then

$$\boldsymbol{S} = -\frac{k_0^2}{4\pi}\left\{\hat{k}^s \times \hat{k}^s \times [l\boldsymbol{P} \cdot \hat{a}] + \hat{k}^s \times [l\boldsymbol{M} \cdot \hat{b}]\right\}\frac{\sin U}{U}$$

where $\boldsymbol{P}$ and $\boldsymbol{M}$ are the tensors previously defined. As expected, for large $k_0 l$ the scattering decreases rapidly away from the forward cone $\hat{k}^s \cdot \hat{z} = \cos\beta$.

VI. Concluding Remarks

The preceding analysis provides an extension of Rayleigh scattering theory to cylindrical dielectric bodies whose transverse dimensions are small compared to the wavelength, but whose length is much greater than λ_0. The results are strikingly similar to those for bodies all of whose dimensions are much less than λ_0 [2], and for a circular cylinder of infinite length, the polarization tensor elements normalized to the cross section area A are identical to the elements for a thin prolate spheroid (or "rod") when normalized to the volume V. Of course, for a cylinder of finite length, $V = lA$, and apart from the factor $\sin U/U$, the same formulas are applicable for $l >> \lambda_0$ and $l << \lambda_0$.

Qualitatively, the variation of P_{xx}/A and P_{yy}/A as functions of ϵ' for fixed ϵ'' is similar for all four cylinder cross sections considered, but there are significant quantitative differences. For a semicircle, for example, the normalized elements differ by almost a factor 2 from those

for a circle, and such shape dependence is greater than that typical of a small body in the Rayleigh region. It would appear that accurate modeling of the cross section is more important when $l >> \lambda_0$, and for remote sensing applications, we note that many pine needles are almost semicircular.

References

[1] J. B. Keller, R. E. Kleinman, and T. B. A. Senior, "Dipole moments in Rayleigh scattering," *J. Inst. Math. Appl.*, vol. 9, pp. 14–22, 1972.

[2] R. E. Kleinman and T. B. A. Senior, "Rayleigh scattering," in *Low and High Frequency Asymptotics*, V. K. and V. V. Varadan, Eds. Amsterdam: North-Holland, 1986, pp. 1–70.

[3] K. Mei and J. Van Bladel, "Low-frequency scattering by rectangular cylinders," *IEEE Trans. Antennas Propagat.*, vol. AP-11, pp. 52–56, 1963.

[4] G. T. Ruck, D. E. Barrick, W. D. Stuart, and C. K. Krichbaum, *Radar Cross Section Handbook, Vol. 1*. New York: Plenum, 1970.

[5] T. B. A. Senior, K. Sarabandi, and F. T. Ulaby, "Measuring and modeling the backscattering cross section of a leaf," *Radio Sci.*, vol. 22, pp. 1109–1116, 1987.

[6] T. B. A. Senior and K. Sarabandi, "Scattering models for point targets," in *Radar Polarimetry for Geoscience Applications*, F. T. Ulaby and C. Elachi, Eds. Dedham, MA: Artech, 1990.

[7] J. A. Stratton, *Electromagnetic Theory*. New York: McGraw-Hill, 1941.

[8] L. Tsang, J. A. Kong, and R. T. Shin, *Theory of Microwave Remote Sensing*. New York: Wiley, 1985.

[9] J. Van Bladel, "Low-frequency scattering by cylindrical bodies," *Appl. Sci. Res.*, vol. 10B, pp. 195–202, 1963.

*

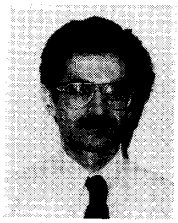

Kamal Sarabandi was born in Tehran, Iran, on November 4, 1956. He received the B.S. degree in electrical engineering from Sharif University of Technology, Tehran, Iran, in 1980. From 1980 to 1984 he worked as a Microwave Engineer in the Telecommunication Research Center in Iran. He entered the graduate program at the University of Michigan, Ann Arbor, in 1984 and received the M.S.E. degree in electrical engineering in 1986, and the M.S. degree in mathematics and Ph.D. degree in electrical engineering in 1989.

He is presently an Assistant Research Scientist in the Department of Electrical Engineering and Computer Science at the University of Michigan. His research interests include electromagnetic scattering and microwave remote sensing.

Dr. Sarabandi is a member of the Electromagnetics Academy.

*

Thomas B. A. Senior (SM '66–F'72) received the M.Sc. degree in applied mathematics from the University of Manchester (England) in 1950, and the Ph.D. degree in research from Cambridge University in 1954.

In 1952 he was appointed as an Established Scientific Officer and accepted a position with the Ministry of Supply at the Radar Research and Development Establishment (now the Royal Radar Establishment) at Malvern, England. In 1955 he was promoted to Senior Scientific Officer. He joined the Radiation Laboratory, University of Michigan, Ann Arbor, in June 1957, where he was appointed Professor of Electrical Engineering and Computer Science in 1969. He served as Director of the Radiation Laboratory from 1975 to 1986, acting Department Chairman in 1987, and has been Associate Chairman of the Department since 1985. His primary interests are in the study of diffraction and propagation of electromagnetic waves, with applications to physical problems.

Dr. Senior has been an Associate Editor for *Radio Science* and served as Editor from 1973 through 1978, and is now an Associate Editor for *Electromagnetics*. He is Chairman of Commission B of the International Union of Radio Science, the past Chairman of the U.S. National Committee for URSI and served as Chairman of the U.S. Commission B. He is a member of Sigma Xi, Tau Beta Pi, and Eta Kappa Nu, and is listed in *American Men and Women of Science*.